J. MATER. CHEM., 1995, 5(8), 1147–1150

MoO_3 Thin Films prepared *via* MOCVD from a Volatile Molybdenyl Complex†

B. Ballarin, E. Brescacin, G.A. Rizzi and E. Tondello*

Centro di Studi sulla Stabilità e Reattività dei Composti di Coordinazione del CNR, Dipartimento di Chimica Inorganica Metallorganica ed Analitica, Via Marzolo 1, Università di Padova, 35131 Padova, Italy

A volatile molybdenyl complex of formula $MoO_2(dpm)_2$ has been studied as a precursor for MOCVD of MoO_3 films. Qualitative indications on the possible decomposition path were obtained by mass spectrometry and thermal analysis. Good quality films were deposited using Pt and Si(100) as substrates. The films were characterised by X-ray photoelectron spectroscopy (XPS), X-ray diffraction (XRD), scanning electron microscopy (SEM), IR and UV–VIS spectroscopies.

Molybdenum oxide MoO_3, like many transition-metal oxides, can have several applications. It is commonly used as a catalyst,[1] but it has been employed in the synthesis of layered intercalation compounds[2] and, when prepared as a thin film, it can be used as the 'active' material in electrochromic devices[3] and gas sensors.[4] Molybdenum oxide films can be prepared by different techniques like electrodeposition,[5] vacuum evaporation directly from MoO_3,[6] plasma enhanced CVD from MoF_6,[7] the sol–gel method[8] and thermal oxidation of Mo films.[3,9] Among the many available deposition methods, metal-organic chemical vapour deposition (MOCVD) techniques offer many potential attractions for thin-film growth and, ultimately, device fabrication. The main advantages are a simplified apparatus which does not require a high vacuum and which allows relatively high reactant gas partial pressures during film growth, relatively low deposition temperatures and, most importantly, adaptability to large-scale deposition for production purposes.

To our knowledge, MOCVD of MoO_3 films has never been performed starting from Mo compounds in high oxidation states, which already contain the Mo—O bond: the films are usually obtained using $Mo(CO)_6$ as the precursor and by oxidising the resulting metallic film, but this method makes it difficult to obtain samples with low carbon contamination. This article reports the results on the use of the molybdenyl compound of formula $MoO_2(dpm)_2$ (Hdpm = 2,2,6,6-tetramethylheptane-3,5-dione) as a precursor for the deposition of MoO_3 films. Complexes containing β-diketonate ligands are commonly used for the deposition of oxide films,[10] but there are few examples of precursors of formula MO_xL_y (L = β-diketonate or similar ligands).[11] There are some possible advantages when using precursors of this type. The first one is a drastic reduction of carbon contamination in the film (absence of Mo—C bonds in the precursor). A further advantage is the presence of Mo in a high oxidation state bonded to O atoms that do not belong to the ligands (Mo=O double bonds). It is likely that a compound of this type will not readily follow a thermal decomposition path implying the breaking of the Mo=O bonds. As a consequence, it is possible to have the direct deposition of a metal oxide (Mo_xO_y) species that may not require a further oxidation process. Moreover, this opens the possibility of producing films on substrates which are normally unsuitable when depositing MoO_3 by oxidation of metallic Mo films. Indeed, substrates such as Si usually give high interdiffusion through a metallic layer, with the possible formation of different phases and compounds, so that it is virtually impossible to obtain pure oxide films.[12]

† Work supported in part by the Ministero per l'Università e la Ricerca Scientifica e Tecnologica (MURST).

Results and Discussion

The precursor was prepared starting from ammonium molybdate following a slightly modified procedure from the literature,[13] and was characterised by standard elemental, IR and NMR spectroscopic analyses. The complex in the solid state could be easily manipulated in air and decomposed slightly only if exposed to direct sunlight for several hours. In order to optimise the conditions for the obtention of deposits, we performed a thermal analysis on the precursor. We studied the decomposition path in both N_2 and O_2 flows by real-time FTIR spectroscopic identification of the volatile pyrolysis products. The thermograms were difficult to interpret since the decrease in weight was partly due to sublimation of the compound. By using a sufficiently high-temperature scan rate it was possible to reduce the weight loss by sublimation so that variations in the thermogram slope caused by decomposition processes could be clearly distinguished; however, no quantitative measurements could be deduced from the thermogravimetry (TGA) curves and only qualitative information on the decomposition paths could be achieved by FTIR identification of the volatile pyrolysis products. Two completely different decomposition paths were identified: the first, obtained in an N_2 flow, corresponds to the presence of vapours of the unaltered complex and, at higher temperatures (*ca.* 300 °C), to the free protonated ligand (Hdpm) and water vapour; the second shows the presence of the free ligand mixed with CO_2 at much lower temperatures (*ca.* 200 °C) and, by further increasing the temperature, of unidentified decomposition products with CO and H_2O vapours. These data demonstrate the remarkably high stability of the precursor in an N_2 atmosphere and its tendency to follow a decomposition path that always implies the loss of a protonated ligand. The main difference between pyrolysis in N_2 and O_2 is the temperature at which this process begins. It is obvious that O_2 burns the Hdpm ligand, as confirmed by the presence of CO_2, and therefore greatly favours the decomposition process. In order to acquire further information on the possible fragmentation paths of the precursor, we performed an electron impact mass spectrum (EI-MS), reported in Fig. 1. The presence of an abundant molecular ion (m/z 490) demonstrates that the complex has good stability under the conditions used for its vaporisation (*ca.* 100 °C). These data also confirm the tendency towards ligand loss leading to the formation of bare MoO_2 neutral species as indicated by: (*a*) the presence of the ions m/z 433 and 307; (*b*) the absence of charged MoO_2 species; and (*c*) the formation of protonated dpm ions (m/z 184). The dpm ions can be generated by a unimolecular dissociation of the molecular ion of the complex, which involves the rearrangement of a hydrogen atom or the ionization of the pyrolysis product of the complex.

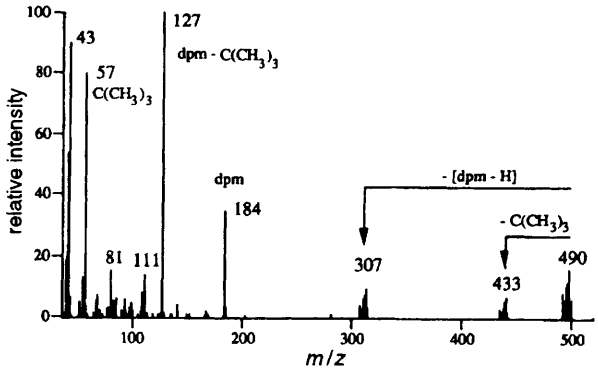

Fig. 1 EI mass spectrum of $MoO_2(dpm)_2$

The deposition of the films was performed in a simple cold wall reactor using a resistively heated susceptor. The precursor showed sufficient volatility to give a considerable deposition rate when heated at temperatures in the range 80–90 °C, while the onset of deposition was found at a substrate temperature of 350 °C. Deposits were obtained on substrates such as polycrystalline Pt, Si(100) wafers and SiO_2, at temperatures ranging from 350 to 430 °C in an oxygen flow. When Ar was used as the carrier gas, no appreciable deposit was obtained (checked by XPS). The O_2 flow rate greatly influenced the growth rate and the morphology of the films. We obtained reflective films with particle sizes in the 100–300 nm range only by using flux rates of 400 sccm (standard cubic centimetres per minute) or higher and a pressure of 6 mbar. Larger crystallites were obtained with lower flow rates. The as-grown samples were always blue in colour. As soon as the precursor flow was stopped and the oxygen pressure was increased to 12 mbar, the blue colour of the films started to bleach out and after several minutes the samples became almost transparent. After further thermal treatment in air at 450 °C for 6 h the samples became totally transparent. The thickness of the films deposited on Si(100) (determined by SEM) with an O_2 flow rate of 490 sccm and a substrate temperature of 430 °C was *ca.* 1.5 μm corresponding to a growth rate of 190 Å min^{-1}. The films deposited on Pt and Si(100) also showed good adhesion properties as verified by the scotch tape test. The samples were characterised using several techniques to determine their composition, structure and morphology.

The XP spectra of the annealed samples, recorded using a monochromatized Al-Kα source, showed the Mo 3d doublet at 232.75 eV with a full width at half maximum (FWHM) of 1.2 eV. The O 1s peak was found at 530.5 eV. Both values are in accordance with literature data.[14] The Mo 3d signal of films grown with 2 mbar oxygen pressure had a shoulder at *ca.* 230 eV which confirms the presence of Mo species in lower oxidation states. This behaviour was also observed for samples grown at higher pressures, but in this case the Mo 3d peak was simply broadened and no resolved shoulder could be identified. This fact is not unexpected because the blue colour shown by the as-grown samples, with different intensities depending on the growth conditions (O_2 flow rate and pressure), can be easily ascribed to the presence of Mo^{IV} and Mo^{V} species. The thermal treatment is therefore necessary to obtain samples with uniform properties. The films were slightly contaminated with carbon on the surface; however, a depth profile analysis showed that the carbon content in the films decreased to 1–2% as soon as the outermost layers were sputtered away. In Fig. 2 we report the Mo 3d doublet for the films grown on Pt and the depth profile relative to the sample after the annealing treatment. The oxygen content

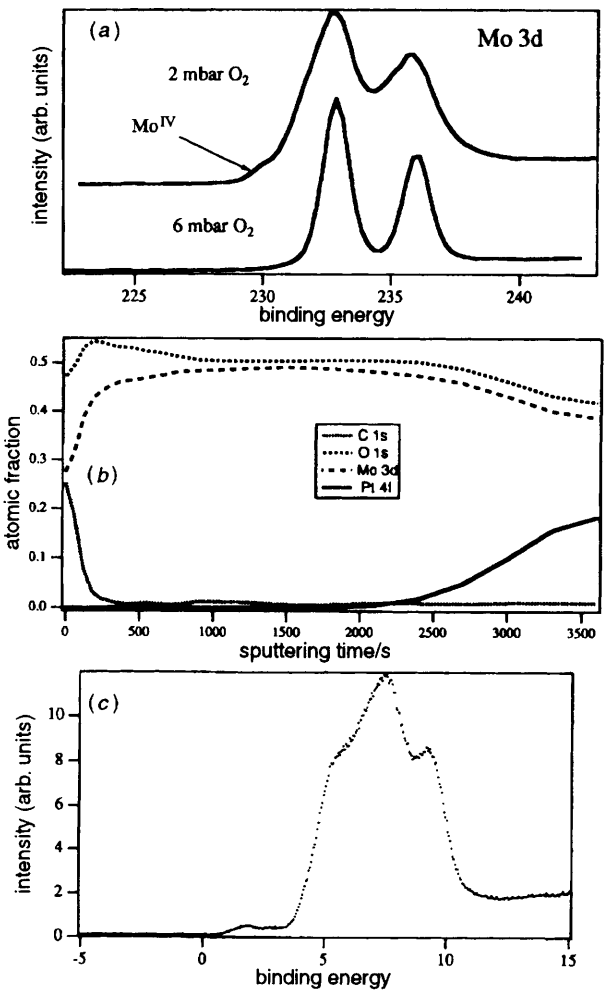

Fig. 2 (*a*) Mo 3d XPS peak from sample grown on Pt. The upper spectrum refers to a sample grown with an O_2 pressure of 2 mbar; the lower one refers to a sample grown with an O_2 pressure of 6 mbar after thermal treatment. (*b*) XPS depth profile of a film grown on Pt (the higher atomic fraction of Mo along the profile is due to a partial reduction of the surface caused by ion bombardment). (*c*) XPS valence band.

found in the samples, after thermal treatment, was always slightly lower than the expected value for perfectly stoichiometric MoO_3 with an average value of 73.4% (75% expected). The XPS results for MOCVD of MoO_3 are summarised in Table 1.

In order to gain some information about the presence of oxygen vacancies in the films we recorded the XPS valence band for the samples grown on Pt and Si(100) after thermal treatment. In both cases the valence band showed three main features at 9.3, 7.4 and 5.5 eV corresponding to the O 2p band and a very weak signal at *ca.* 1.8 eV (see Fig. 2). This weak extended tail can be assigned to oxygen vacancies or to different combinations of the metal d orbitals with the 2p orbital of oxygen.

The reflectance IR spectrum of a sample deposited on Pt is reported in Fig. 3. For comparison, the spectrum of MoO_3

Table 1 XPS data for MoO_3 films after thermal treatment

substrate	Mo/ atom%	O/ atom%	Mo $3d_{5/2}$/ eV	O 1s/ eV
Pt	26.3	73.7	232.75	530.5
Si(100)	26.9	73.1	232.75	530.5

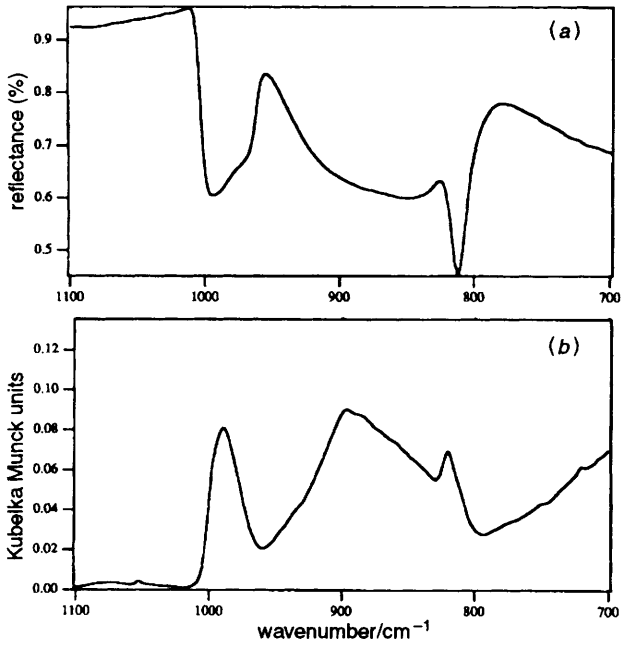

Fig. 3 (*a*) IR reflectance spectrum of MoO_3 film deposited on Pt. (*b*) IR diffuse reflectance spectrum of MoO_3 powder.

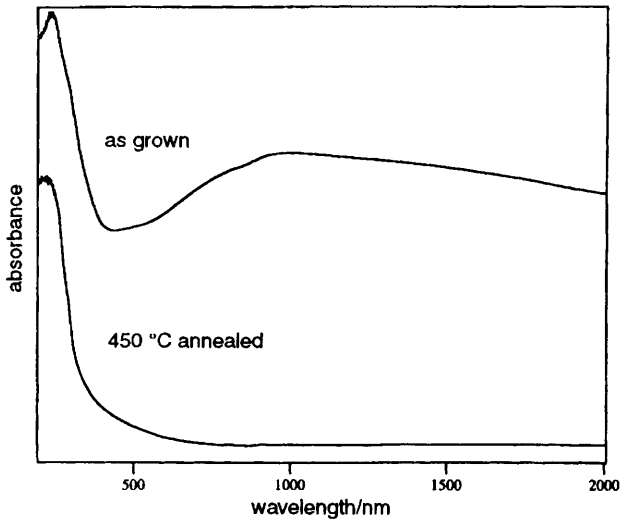

Fig. 4 UV–VIS spectra of films grown on SiO_2; the upper curve refers to an as-grown sample while the lower curve corresponds to the same sample after annealing in air

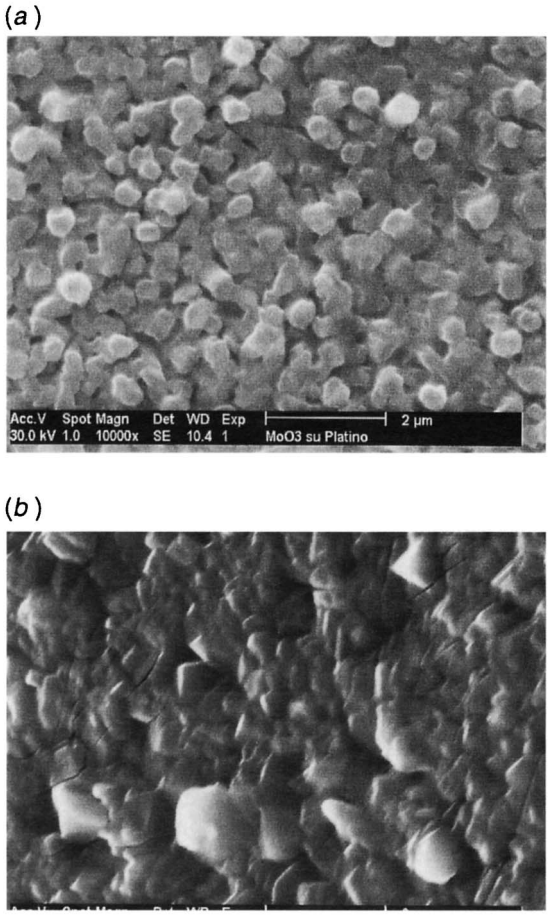

Fig. 5 Scanning electron micrographs of films deposited on Pt (*a*) and Si(100) (*b*)

powder is also shown. There is a remarkably high similarity between the two spectra. The IR spectra of the films show an intense peak at 993 cm^{-1} with a shoulder at 972 cm^{-1}, followed by a broad band with a maximum at 854 cm^{-1} and a peak at 812 cm^{-1}. The corresponding peaks in the diffuse reflectance spectrum are found at 990, 896 and 820 cm^{-1}, respectively.[15] The sharp band at *ca.* 990 cm^{-1} can be regarded as being due to the stretching vibrations of the independent Mo–O groups while the two bands at longer wavelengths are attributed to the two different (Mo–O–Mo) continuous structures. Similar results were obtained upon recording the spectra in absorbance mode for the films deposited on Si(100).

We recorded the UV–VIS spectra (in absorbance mode) of a sample deposited on SiO_2 before and after the thermal treatment. The spectrum of the as-grown film shows the absorption edge at *ca.* 400 nm with its maximum at 242 nm and a shoulder at 293 nm. The spectrum also shows a very broad absorption in the visible region extending from 600 to almost 2000 nm (see Fig. 4). The annealed sample does not show any bands in the visible region, while the absorption extending from 400 nm sharpens and shows bands at 292 and 230 nm. These results are in agreement with the absorption spectra of thin films of MoO_3 deposited by vacuum evaporation followed by an annealing procedure in O_2 at 300 °C.[16] It is clear that, as evidenced by the XPS measurements, the as-grown films contain Mo in lower oxidation states (V and IV). The thermal treatment seems to be effective in the formation of Mo^{VI} species since not even weak absorptions are detected in the visible part of the spectrum. As expected, the annealing procedure increased the crystallization of the sample, as can be deduced from the appearance of a more resolved fine structure in the absorption band starting at 400 nm.

The morphology of the films is shown by the SEM images presented in Fig. 5, referring to the samples deposited on Pt and Si(100) obtained using the same deposition parameters (O_2 flow 490 sccm; pressure 6 mbar; precursor temperature 80 °C). The film deposited on Pt shows a rough texture with an average grain size of 0.3–0.5 μm. A different morphology is found for the samples grown on Si(100): the grain size is slightly larger and the shape of the microcrystals is completely different.

The XRD data for the sample grown on platinum are identical to the reported powder pattern,[17] thus confirming that the sample consists of a single molybdite phase. However, the samples grown on Si(100) and SiO_2 have a preferential orientation of the crystallites along the *c* axes.

Conclusions

The deposition rate, taking into account the low vapour pressure showed by the precursor, can be reasonably assumed to be feed-rate limited. When using low flow rates a lower number of nucleation sites on the surface is formed, the oxidation of Mo_xO_y species is favoured and larger crystallites are obtained. It is obvious that the oxygen uptake by the system is due to the precursor decomposition (combustion of the ligand) and to the oxidation of the Mo_xO_y species where the metal centre can possess oxidation states ranging from IV to VI. The differences in the morphology of the films when using Pt or Si as substrates can be obviously ascribed to the different texture of the substrate (polished polycrystalline Pt and Si single crystal).

In summary, MOCVD of high-purity crystalline MoO_3 has been demonstrated. The precursor can be easily obtained and manipulated, and shows a sufficiently high volatility to have useful deposition rates. The use of a molybdenyl precursor allows the formation of deposits with a low carbon content. The presence in the precursor of an already oxidised metal centre avoids possible intermixing of metallic Mo on substrates like Si or other metals.

Experimental

Synthesis of $MoO_2(dpm)_2$

Concentrated HNO_3 was added dropwise to a 25 ml (1:1) ethanol–water solution of $(NH_4)_6Mo_7O_{24}\cdot 4H_2O$ (0.5 mmol) until complete dissolution of molybdic acid occurred. The resulting yellow solution was then mixed with 1.5 ml (7.2 mmol) of 2,2,6,6-tetramethylheptane-3,5-dione under vigorous stirring. The insoluble organic phase turned deep yellow after 30 min, and was extracted with benzene. After solvent and ligand excess evaporation under vacuum, a yellow solid was obtained. All procedures were carried out while avoiding exposure of the reagents to light. Mp 104–105 °C. Elemental analysis: Calc. for $C_{22}H_{38}MoO_6$: C, 53.44; H, 7.75. Found: C, 53.63; H, 7.69%. IR ν/cm^{-1} (DRIFT): 938 (s) and 913 (s). ^1H NMR δ ($CDCl_3$, Me_4Si as reference): 1.07 (s, 9 H), 1.20 (s, 9 H), 5.97 (s, 2 H).

Film Deposition

Owing to its moderate volatility, and to avoid condensation in the tubing and valve system, the precursor was heated in a small crucible inside the reactor by heating tapes and controlling its temperature with a thermocouple. The carrier flux was measured and controlled with an MKS mass flow controller and the pressure was measured with a capacitance manometer. The deposition was continued until no precursor was left in the crucible. The polycrystalline Pt substrate was mirror-polished to 1 μm, rinsed with doubly distilled water and washed with ethanol in an ultrasonic bath. The Si(100) wafer was washed with warm trichloroethene in an ultrasonic bath.

Instrumentation

A Perkin-Elmer Φ 5600ci spectrometer with monochromatized Al-Kα radiation (1486.6 eV) was used for the XPS analyses. The working pressure was less than 1.8×10^{-9} mbar. The spectrometer was calibrated by assuming the binding energy (E_b) of the Au $4f_{7/2}$ line at 83.9 eV with respect to the Fermi level. As an internal reference for the peak positions the C 1s peak of hydrocarbon contamination was assumed at 284.8 eV. The standard deviation in the E_b values of the XPS lines was 0.10 eV. After a Shirley-type background subtraction, the raw spectra were fitted using a non-linear least-squares fitting program adopting Gaussian–Lorentzian peak shapes for all the peaks. The atomic compositions were evaluated using sensitivity factors as provided by Φ V5.4A software. Depth profiles were carried out by Ar^+ sputtering at 2.5 keV, 0.4 μA cm^{-2} beam current density with an argon partial pressure of 5×10^{-8} mbar.

IR measurements were performed on an FTIR Bruker IFS 66 instrument and the UV–VIS data were recorded on a Varian Spectrophotometer Cary 5E.

TG analysis of the precursor was performed on a Perkin-Elmer Thermobalance TGS-2 in both oxygen and nitrogen flows with a heating rate of 20 °C min^{-1}. Mass spectra were obtained using a VG ZAB 2F mass spectrometer with a direct introduction system (E_I = 70 eV, mass resolution = 5000). SEM micrographs were obtained on a XL 40 La B99 scanning electron microscope.

XRD measurements were performed on a Philips MPD 1880 powder diffractometer with graphite monochromated Cu-Kα radiation in the Bragg–Brentano parafocusing geometry. The sample holder did not contribute to the diffraction patterns.

We thank Dr. U. Vettori for mass spectrometry measurements and useful discussions; we thank Prof. G. Favero for TG measurements, and Dr. P. Guerriero for SEM data.

References

1 H. H. Kung, *Transition Metal Oxides: Surface Chemistry and Catalysis*, Elsevier, Amsterdam–Oxford–New York–Tokyo, 1989.
2 M. G. Kanatzidis and T. J. Marks, *Inorg. Chem.*, 1987, **26**, 783; E. Lalik, W. Kolodziejski, A. Lerf and J. Klinowski, *J. Phys. Chem.*, 1993, **97**, 223.
3 A. Donnadieu, D. Davazoglou and A. Abdellaoui, *Thin Solid Films*, 1988, **164**, 333.
4 A. M. Azad, S. G. Mhaisalkar, L. D. Birkefeld, S. A. Akbar and K. S. Goto, *J. Electrochem. Soc.*, 1992, **139**, 2913.
5 D. Belanger and G. Laperriere, *Chem. Mater.*, 1990, **2**, 484; M. Tölgyesi and M. Novak, *Jpn. J. Appl. Phys.*, 1993, **32**, 93; J. N. Yao, B. H. Loo, K. Hashimoto and A. Fujishima, *Ber. Bunsen-Ges. Phys. Chem.*, 1991, **95**, 557.
6 J. N. Yao, B. H. Loo, K. Hashimoto and A. Fujishima, *Ber. Bunsen-Ges. Phys. Chem.*, 1991, **95**, 554; J. Yao, B. H. Loo and A. Fujishima, *Ber. Bunsen-Ges. Phys. Chem.*, 1990, **94**, 13.
7 M. Anwar and C. A. Hogarth, *J. Mater. Sci.*, 1990, **25**, 4918.
8 Y. Tokako, B. Nobuyoshi and Y. Koichi, *Nippon Kagaku Kaishi*, 1988, **9**, 1525.
9 T. Kodas and M. Hampden Smith, *The Chemistry of Metal CVD*, VCH, New York, 1994, p. 390 and references therein.
10 D. L. Schulz and T. J. Marks, *Adv. Mater.*, 1994, **6**, 719.
11 E. Kikuchi, K. Itoh and A. Fujishima, *Nippon Kagaku Kaishi*, 1987, **11**, 1970.
12 W. Schröter, *Materials Science and Technology*, vol. 4, *Electronic Structure and Properties of Semiconductors*, ed. R. W. Cahn, P. Haansen and E. J. Kramer, VCH, Weinheim, 1991, pp. 422–438.
13 T. J. Pinnavaia and W. R. Clements, *Inorg. Nucl. Chem. Lett.*, 1971, **7**, 1127; H. Gehrke Jr. and J. Veal, *Inorg. Chim. Acta*, 1969, **3–4**, 623.
14 B. Brox and I. Olefjord, *Surf. Interface Anal.*, 1988, **13**, 3.
15 See, for example: *Gmelin Handbuch der Anorganischen Chemie*, vol. 53 B1, Springer–Verlag, Berlin, 1975, p. 101.
16 S. K. Deb and J. A. Chopoorian, *J. Appl. Phys.*, 1966, **37**, 4818.
17 Pattern 35–609 on JCPDS–ICDD (Joint Committee on Powder Diffraction Standards–International Center for Diffraction Data).

Paper 5/00720H; *Received 7th February*, 1995